Egyptian Journal of Chemistry

http://ejchem.journals.ekb.eg/

Bioengineering of Zinc Oxide Nanoparticles As Therapeutics for Immunomodulatory and Antimicrobial Activities

Gamal M. El-Sherbiny [1], Amir R. Ali [2], and Diaa M. Ali [1], Ahmad S. El-Hawary[1], Ahmed A. Askar [1]

[1]*Botany and Microbiology Department, Faculty of Science (Boys), Al-Azhar University, Cairo, 11884, Egypt.*
[2]*Applied-Science & Robotics Laboratory for Applied-Mechatronics (ARAtronics Lab.); Mechatronics Engineering Department, German University in Cairo, New Cairo 11835, Egypt.*

ABSTRACT

In the present work, eco-friendly biosynthesis of zinc oxide nanoparticles (ZnONPs) and their immunostimulatory and antimicrobial activity were investigated. Streptomyces rochei, the ZnONPs manufacturer, were isolated and identified. The morphology and characterization of ZnONPs using UV-Vis, DLS, TEM, and XRD, were investigated. The results showed that the spherical shape of ZnONPs was with a mean diameter of about 36nm. The viability of the HFB-4 and Vero cells was decreased to 42 and 46% respectively after treatment with a dose of 16µl/ml of ZnONPs. ZnONPs showed a significant immunostimulatory effect with 137.2 ± 0.18% and increased CD4+ and CD8+ lymphocytes level with 85.2 ± 0.07% and 25.3 ± 0.03%, respectively. Also, they exhibited an antimicrobial activity against both Gram-negative, positive bacteria and fungi with inhibition zone ranging from 16.0 to 28.0 mm and MIC ranging from 8.67 to 125.0 µg/ml. This study highlights that ZnONPs strongly stimulate immune system and have antimicrobial activities.

Keywords: *Streptomyces rochei, Biosynthesis of zinc oxide nanoparticles, Cytotoxicity, Immunomodulatory, Antimicrobial activity*

1. Introduction

For more than a couple of decades, nanotechnology has been continuing as a trending scientific sector deals with material in nanoscale (1 nm – 100 nm) [1]. It shows a helpful solution for too many problems in many fields including electronics, energy, textiles, geotechnical engineering, chemical industries, medicine and agronomy [2-4]. Among nanoscale metals, ZnONPs are precious oxides because they are marked with distinctive physicochemical properties. Moreover, therapeutically they showed antitumor, antioxidant, antidiabetic and antimicrobial activities [5-7].

Engineered zinc oxide nanoparticles display versatility, unique physicochemical characteristic that has a huge medical application and are broadly used in sunscreens and cosmetics, due to their excellent UV filtering characters [8]. Interestingly, despite their elevated production volumes and the wide application base, there is always a prospect of accidental exposure to their NPs. This can result in unpremeditated side effects that are caused due to the predisposition of these materials to demonstrate biological reactivity [9]. Zinc is one of the vital elements for humans, animals, and microorganisms. Zinc has a key role in maintaining crucial cellular processes including DNA repair, oxidative stress, DNA replication and cell cycle progression [10]. Zinc oxide nanoparticles (ZnONPs) have gained a tremendous attention due to their unique properties. They have a high absorption rate, lower toxicity [11], better biocompatibility and bioavailability compared to their conventional Zn sources [12]. The cytotoxicity of zinc oxide nanoparticles has been previously recorded in many *in vitro* test systems involving lung epithelial cells, immune cells, colorectal epithelial adenocarcinoma cells and keratinocytes [13-18]. Other studies have revealed that zinc oxide nanoparticles can cause cytotoxicity via apoptosis [19-21] and genotoxicity as well [22-24]. Despite some discrepancy reports, the essential paradigm explaining zinc oxide nanoparticles' cytotoxicity is due to their inclination to dissolve, resulting in releasing of Zn^{2+} ions, with a linked generation of reactive oxygen species (ROS) [17,25]. Extracellular dissolution of zinc oxide nanoparticles and releasing of Zn^{2+} ions have been inducing cell death in human T-cell leukemia cells [26] and mouse macrophage (Ana-1) cells [27].

Several studies showed a wide range of biological and therapeutic activities of zinc

*Corresponding author e-mail: gamalelsherbiny1970@yahoo.com
Receive Date: 28 April 2022, **Revise Date:** 13 June 2022, **Accept Date:** 19 June 2022, **First Publish Date:** 19 June 2022
DOI: 10.21608/EJCHEM.2022.136366.6008

nanoparticles including antibacterial, antiprotozoal, antioxidant and anticancer [10, 28-30]. Numerous mechanisms have been introduced to explain the antibacterial effect of ZnONPs [31]. The positively charged surface of ZnONPs and their surface polarity can affect their bacterial resistance mechanism. The interaction between positively charged Zn^{+2} NPs ions and negatively charged bacteria resulted in the firm attachment of the ions to bacteria and induced their death [32,33]. Many nanomaterials exhibit antitumor characteristics *in vitro* but also exert tumor-promoting influence *in vivo* because of the dispersed anticancer immune system [34]. Therefore, it is also possible that increased exposure to ZnONPs may cause immunomodulation. Immunomodulation is preferred to prevent and treat diseases and is used as a vaccine adjuvant and antiallergy therapeutic [35]. Biological synthesis provides an eco-friendly and cost-effective method. An alternative approach for the synthesis of metal nanoparticles is to apply biomaterials such as plants, microorganisms encompassing groups such as bacteria, yeasts, fungi, and actinomycetes as manufactories [36]. In comparison with other microorganisms, actinomycetes could be used as the most efficient biotechnological agent for the sustainable production of nanoparticles. Actinomycetes are a flexible tolerant, easy and economic biological system that have been used extensively in the industry. Several actinomycetes species were found to synthesize metal nanoparticles [37]. The main aim of the study is the isolation and identification of an actinomycete strain with a potential green synthesis of ZnONPs. Furthermore, characterization, evaluation of cytotoxicity, immunomodulatory and antimicrobial activities of ZnONPs.

2. Materials and methods

2.1. Chemicals

All the media components were from Oxide and chemicals and reagents used in the following experiments were of analytical grade and were used without further purification.

2.2. Isolation and identification of actinomycetes isolates

Soil samples were collected from a place near the Mina Coast region; El-Menia governorate, Egypt in February 2018. Soil samples were collected in sterile airlock polyethylene bags and for isolation of actinomycetes, samples were cultivated on the International Streptomyces Project - 4 (ISP4) agar media. The pure isolates were characterized and identified based on morphological, physiological, biochemical characteristics, and genetic analysis [38-41]. The *Streptomyces* isolates were identified using 16S rDNA sequence analysis. Genomic DNA was extracted from the collected strains at the late exponential growth stage using the protocol of Gene Jet genomic DNA purification kit (Thermo Fisher Scientific, USA K0791) and according to the manufacturer's recommendations. Amplification of 16S ribosomal DNA of the selected isolates was carried out using the primers 27F (5-AGAGTTTGATCCTGGCTCAG-3) and 1495R (5-CTACGGCTACCTTGTTACGA-3) by polymerase chain reaction (PCR). Amplification was conducted using a BIO-RAD PCR System T100 thermocycler (BIO-RAD Laboratories, Hercules, CA, USA) under the following cyclic profile: initial denaturation at 95 °C for 2 min, 30 cycles of denaturation at 95 °C for 1 min, annealing at 54 °C for 30 s, with extension at 72 °C for 2 min and a final extension at 72 °C for 5 min. The PCR product was purified using K0701 Gene JET™ PCR Purification Kit (Thermo Fisher Scientific USA). The partial 16S rDNA sequence of strain was compared using the BLAST program (https://blast.ncbi.nlm.nih.gov/Blast.cgi). Then, identification of the species was performed by comparing the similarity with the prototype strain sequence in the GenBank database. Finally, the phylogenetic tree was constructed using the MEGA software program (version 6.0) [42,43].

2.3. Preparation of cell-free extract

Streptomyces rochei was inoculated in a 250 ml flask containing 50 ml of the liquid basal salts starch-nitrate medium [44]. The medium included the following components (g/l): 2.0, KNO_3; 20.0, starch; 0.5, $MgSO_47H_2O$; 1.0, K_2HPO_4; 0.5, NaCl; 3.0, $CaCO_3$ and 0.01, $FeSO_47H_2O$. Inoculation was done by a disk of 0.4 cm diameter obtained from seven days old culture plates of the examined isolate, then was incubated in a rotary shaker at 200 rpm and 37°C with an initial pH of 7.0 for four days. After an incubation period, actinomycete cells were removed from the suspension by filtration through a 0.44 µm PVDF filter; then, they were centrifuged at 10,000 rpm to remove occasional actinomycetes cells [45].

2.3.1. Biosynthesis of zinc oxide nanoparticles (ZnONPs).

The aqueous solution of 1mM zinc nitrate solution (50 ml) was mixed with the cell-free filtrate (CFF) (50 ml) and the pH was adjusted to 8.5. The mixture was incubated in a rotary shaker at 37 ºC and 200 rpm in the dark for 24h. Control experiments were performed with un-inoculated media and zinc nitrate solution to check the role of actinomycete in nanoparticle synthesis. The zinc ions reduction was examined by sampling about 2ml of the solution at time intervals and monitoring the UV–Vis spectra by using a UV–Vis spectrophotometer (JASCO V-560). In each reaction vessel, the resulted color change by formation of a white suspension was observed. ZnONPs suspension was further centrifuged at 12,000

rpm for 30 min, and the collected precipitate pellet was dried and weighed [46].

2.3.2. Characterization of biosynthesized ZnONPs.

The optoelectronic properties of the biosynthesized ZnONPs were measured by ultraviolet-visible absorption spectra (UV-vis, Hitachi U-2800) in the range of 200-800 nm. The Fourier transform infrared spectroscopy (FTIR) spectrum of the sample was recorded on an Agilent system Cary 630 FTIR model, Chemistry Department, Faculty of Science, Al-Azhar University, Cairo, Egypt, in the range 400 - 4,000cm^{-1}. The spectral data obtained were compared with the reference chart to identify the functional groups present in the sample. The size and shape of the products were observed by High-resolution transmission electron microscopic (HRTEM) (JEOL 2100 Japan, at National Research Center (NRC), Giza, Egypt). The crystalline structure of the biosynthesized ZnONPs was identified by X-Ray diffraction analysis using the Shimadzu Scientific Instruments (SSI), Kyoto, Japan, with nickel-filter, in the 2h range of 20-90^{o} operated at 40 kv and 30mA. The particle size distribution of ZnONPs was evaluated using Dynamic Light Scattering (DLS) measurement conducted with a Malvern Zetazier Instrument. Measurements were taken in the range between 0.1 and 1000µm. Data obtained were analyzed using Zetasizer software. The XRD and DLS were measured at the National Center for Radiation Research and Technology (NCRRT), Cairo, Egypt.

2.4. *In vitro* cytotoxicity of ZnONPs against normal cells

The cytotoxic activity of ZnONPs was evaluated *in vitro*, using the HFB-4 (normal human melanocytes) and Vero (derived from kidney epithelial cells of African green monkey) cell lines according to Abu-Serie and El-Fakharany [47], in triplicates. The cell viability and proliferative potential based on their metabolic activity were determined with MTT (3-(4,5-dimethyl thiazolyl-2)-2,5-diphenyltetrazolium bromide) assay. The adherent culture medium was replaced by a medium containing different concentrations of 0.0, 1, 2, 4, 8, 16, 32, 64, and 128, µg/ml of ZnONPs and incubated for 24 h. After that, the cells were washed three times with fresh media or cold PBS and incubated with 0.5 mg/ml MTT (Sigma-Aldrich) for 2-5 h. Then MTT solution was removed and 200µl of DMSO was added to each well. The optical density (OD) of each dose was read at 570 nm using a microplate reader (BMG LabTech, Germany). The % cell viability and % cell death were calculated using the following formulas:

$$\% \text{ Cell viability} = \frac{Treat\ cells}{Control\ cells} \text{ X } 100$$

$$\% \text{ Cell death} = \frac{Control\ OD - Sample\ OD}{ControlOD} \text{ X } 100$$

2.5. Determination of immunomodulatory activity:

In vitro intracellular killing activities of biosynthesized ZnONPs were performed according to reported methods of referenced literature [48, 49]. While *in vivo* immunomodulatory involved (Relative immune organs weight and indexes, as well as determining the T lymphocytes subsets (CD4+ and CD8+)) were evaluated. Male laboratory-bred Swiss albino mice (6-8 weeks old) (n =24), weighing 20 ± 2 g were used. They were randomly divided into four groups, the first group received cell-free supernatant (CFS), the second group received ZnONPs 5 µg/ml, the third group received vitamin C (positive control), and the fourth group received saline in a normal diet (negative control) according to reported methods [50-51]. ZnONPs and vitamin C were prepared in water for doses of 5.0 mg/kg body weight and the mixture was vortexed for 5 min at room temperature and after that sonicated at 4 °C for 10 min then orally administered to mice.

2.6. Determination of thymus and spleen indices

After fourteen days of treatments, Swiss albino mice in each group were killed by cervical dislocation. The spleen and thymus were removed and weighed. The organ index was calculated as follows [51].

$$\text{Index (mg per 10g)} = \frac{\text{weight of spleen or thymus (mg)}}{\text{body weight (g)}}$$

This study was approved by the Social Science Ethical Committee of the Faculty of Science, Tanta University, and complied with the Egyptian Code of Conduct for Scientific Practice, National Research Centre, Egypt.

All procedures related to the care and maintenance of the animals were performed according to the international guiding principles for animal research and approved by the Suez Canal University bioethics and animal ethics committee (the approval no. 201505).

2.7. Screening for antimicrobial activity

A Stock solution of biosynthesized ZnONPs (5mg/ml) was prepared in distilled water then the antibacterial activity was determined against *Bacillus subtilis* (ATCC 6633), *Staphylococcus aureus* (ATCC 6538), *Pseudomonas aeruginosa* (ATCC 9027), *Escherichia coli* (ATCC 7839), *Aspergillus niger* 002007(RCMB), *Aspergillus flavus* (ATCC 16883) and *Candida albicans* (ATCC 10231). This assay was performed using the agar well diffusion technique, in which, wells (8 mm) were cut in Muller Hinton agar (Merck Kga A, Germany) plates inoculated with the tested bacteria. Fifty microliters of ZnONPs solution were pipetted into each well. After incubation at 37°C for 24h and 30°C for 5 days, the inhibition zone diameter around each well was measured in mm. Antibiotic paper disks of tetracycline and

amphotericin B were used for comparison in this assay that was carried out according to the Kirby-Bauer method [52].

A atistical Analysis

The means of three replicates and the standard deviation (SD±) were calculated for all obtained results and the data were subjected to analysis of variance. Means share different superscripts are significantly different at (P< 0.05) [53].

3. Results

3.1. identification of the actinomycete producer

After seven days of incubation at 37˚C, pure colonies were isolated on starch casein agar medium and sub-cultured on ISP-4 agar medium. Culture characteristics of actinomycete isolate El-Menia-19 are presented in Table (S1). It exhibited very well to good growth on ISP-3, ISP-4, ISP-5, and ISP-7 media. The color of the aerial mycelium appeared grey to white, while the substrate mycelium fluctuated from beige to yellow. This isolate does not produce soluble pigment on various ISP media. Also, showed moderate growth on ISP-1, ISP-2, and ISP-6 media. Micromorphological characteristics of actinomycete isolate, grown on inorganic salts-starch agar (ISP-4) were investigated under light microscopy Figures 1 (A and B) and exhibited straight shaped mycelium that further differentiated into smooth-surfaced spores and unique morphological characteristics were seen under a scanning electron microscope Figure 2 (C and D). The average diameter of the spores is around 0.10 mm. The spore chain consists of 10-15 spores/chains. The whole-cell hydrolysate of this strain contained LL-d **C** opimelic acid (LL-DAP), and this isolate has a chemo-type I cell wall with no specific sugars could be recognized. Detailed physiological and biochemical properties of the strain are given in the species description in Table (S2). The isolate El-Menia-19 shows cultural similarity with *Streptomyces rochei.* To confirm the identification of the isolated *Streptomyces* species, the 16S rRNA gene sequence of the local isolate was compared to sequences of *Streptomyces* sp. Experimental analysis of the PCR amplification was studied through the agarose gel electrophoresis exhibited a specific 16S rRNA band. The phylogenetic tree Figure (2) showed that the locally isolated strain is closely related to *Streptomyces rochei*, which was constructed using the neighbor-joining method with the aid of the MEGAX tree builder program. Bar 0.20 substitutions per nucleotide position. Multiple sequence alignment was done between the sequences of the 16S rRNA genes of *Streptomyces rochei* and other eight *Streptomyces* sp. and the local isolate. Computer-assisted DNA similar searches against bacterial databases revealed that the 16S rRNA sequence was 99.49% identical to that of *Streptomyces rochei*. The nucleotide 16S rRNA gene sequence was deposited in the NCBI gene bank under accession number MW717421.1

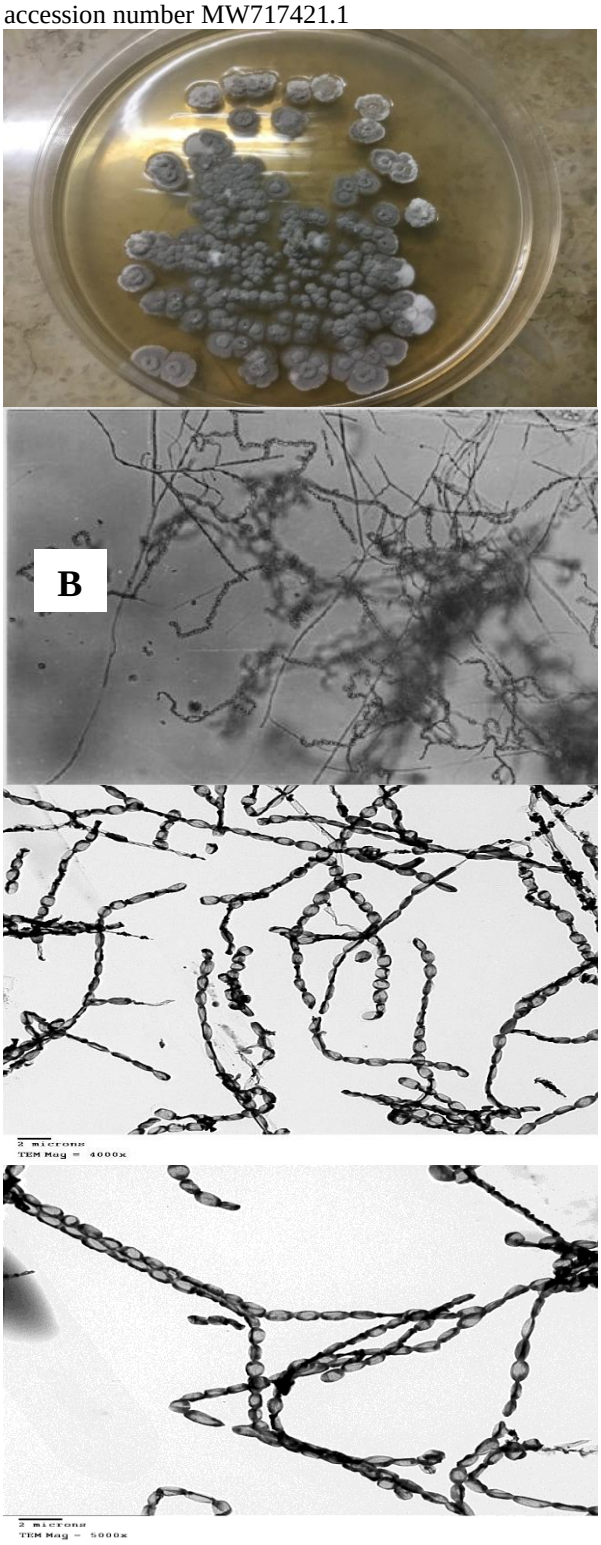

Figure (1): (**A)** growth of actinomycete isolation ISP-4, (**B**) Phase-contrast micrograph showing straight shaped mycelium, (C and D) transmission electron microscopy (TEM) showing straight-shaped mycelium that further differentiated into smooth-surfaced spores.

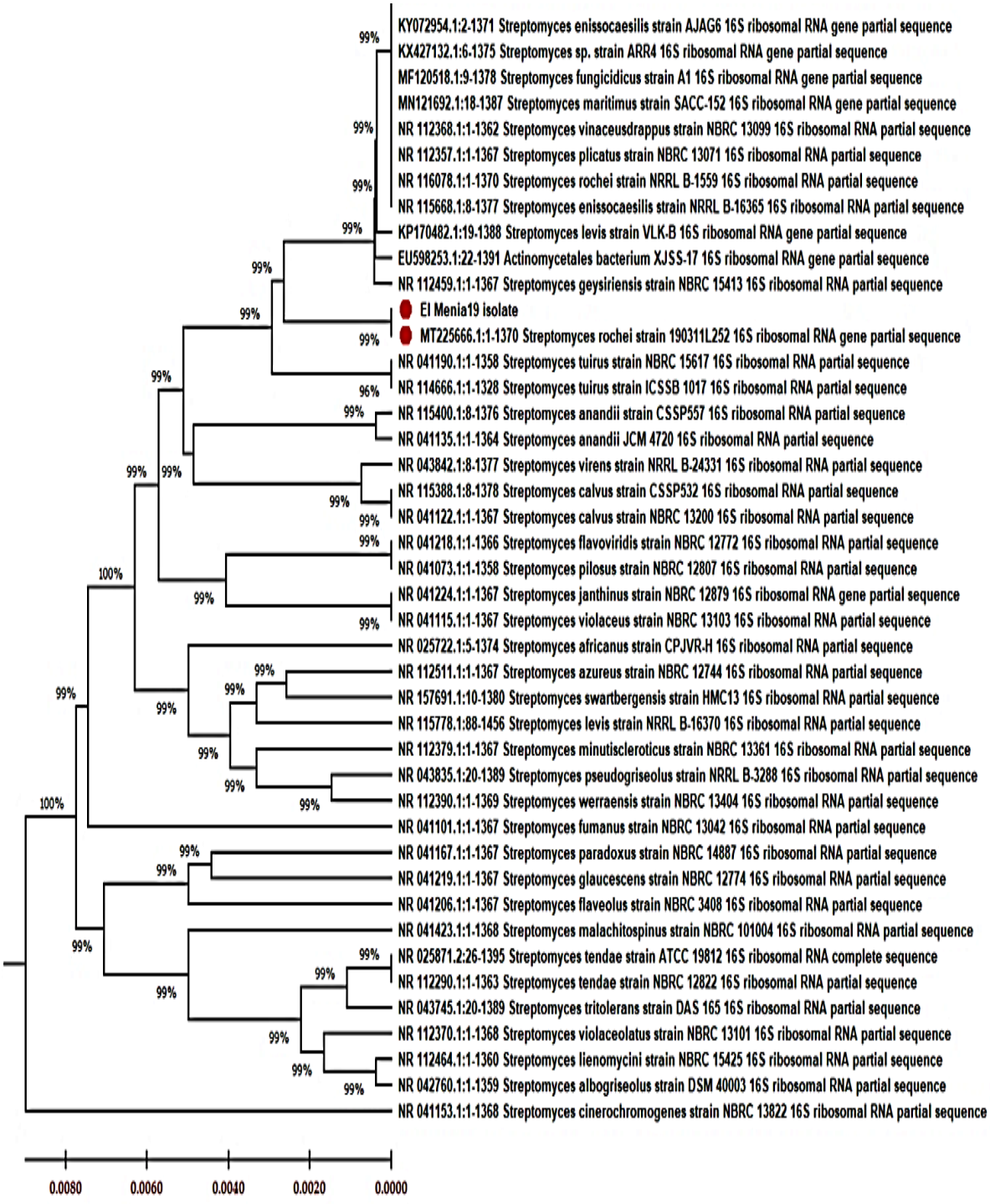

Figure (2): Phylogenetic tree based on partial 16S rDNA sequences, showing the relationship between isolate El_Menia-19 and other species belong to the genus *Streptomyces*. The tree was constructed using the MEGAX and neighbor-joining method.

3.2. Biosynthesis of ZnONPs by *Streptomyces rochei*

The precursor solution of zinc nitrate was reduced by cell-free supernatant (CFS) of *Streptomyces rochei*. The color changed from pale yellow to milky white, indicating the formation of ZnONPs.

3.3. Characterization of Biosynthesized ZnONPs

3.3.1. UV-Visible Spectrophotometer (UV-Vis.).

The dispersion of ZnONPs displays intense colors due to the plasmon resonance absorption. The surface of the metal is like plasma, having free electrons in the conduction band and positively charged nuclei. Therefore, metallic nanoparticles have

the characteristic of the optical absorption spectrum in the UV-visible region. As shown in Figure (3 A), the UV-Visible spectrum of ZnONPs synthesized by active cell-free filtered (CFF) has a spectrum at λ maximum at 455 nm.

3.3.2. Dynamic Light Scattering (DLS)

DLS analysis is mainly used to determine the size of particles in different suspensions. To examine the particle size distribution, DLS was also performed, and its results were compared to the TEM data. The average particle size for ZnONPs was determined by the dynamic light scattering (DLS) method and found to be approximately 36.3 ± 6.8 nm as shown in Figure (3 B).

3.3.3. Transmission Electron Microscopy (TEM)

The transmission electron microscopy (TEM) examination of the solution containing ZnONPs demonstrated spherical particles within nano ranging from 14.52 nm to 36.2 nm with the average mean diameter of 30.75 nm as shown in Figure (3C).

3.3.4. X-Ray Diffraction (XRD).

The crystallinity and crystal phase of the synthesized ZnONPs was examined by XRD. ZnONPs showed peaks with 2θ values identified at 31.841°, 34.507°, 36.324°, 47.592°, 56.634°, 66.426°, 67.983°, 69.091°, and 76.987° corresponding to planes (100), (002), (101), (102), (110), (103), (112), (201) and (202) planes respectively, Figure (3D), confirming that the material has a hexagonal close-packed crystalline structure in space group. The average crystallite size of the ZnONPs was determined using the Debye–Scherrer equation

$$D = \frac{0.9\lambda}{B\cos(\theta)}$$

Where D is the crystal size (nm), λ is the X-ray wavelength (0.1541 nm), β is the full width at half maximum in radians and θ is the diffraction angle at the corresponding lattice plane. The average crystallite size of the ZnONPs was found to be approximately 36 nm, which correlates with the TEM images.

3.4. *In vitro* cytotoxicity of biosynthesized ZnONPs

The biosynthesized ZnONPs from *Streptomyces rochei* were subjected to cytotoxicity on HFB-4 and Vero cells. The dose-dependent effect of ZnONPs against eukaryotic cells was observed. The human HFB-4 viability after treatment with 0, 1, 2, 4, 8, 16, 32, 64 and 128 µg/ ml for 24h ZnONPs was found to be 100, 100, 97, 85, 84, 58, 45, 32 and 20%, while in Vero cells (derived from kidney epithelial cells of African green) was 100, 100, 94, 83, 80, 54, 40, 27 and 15%, respectively (Figure 4).

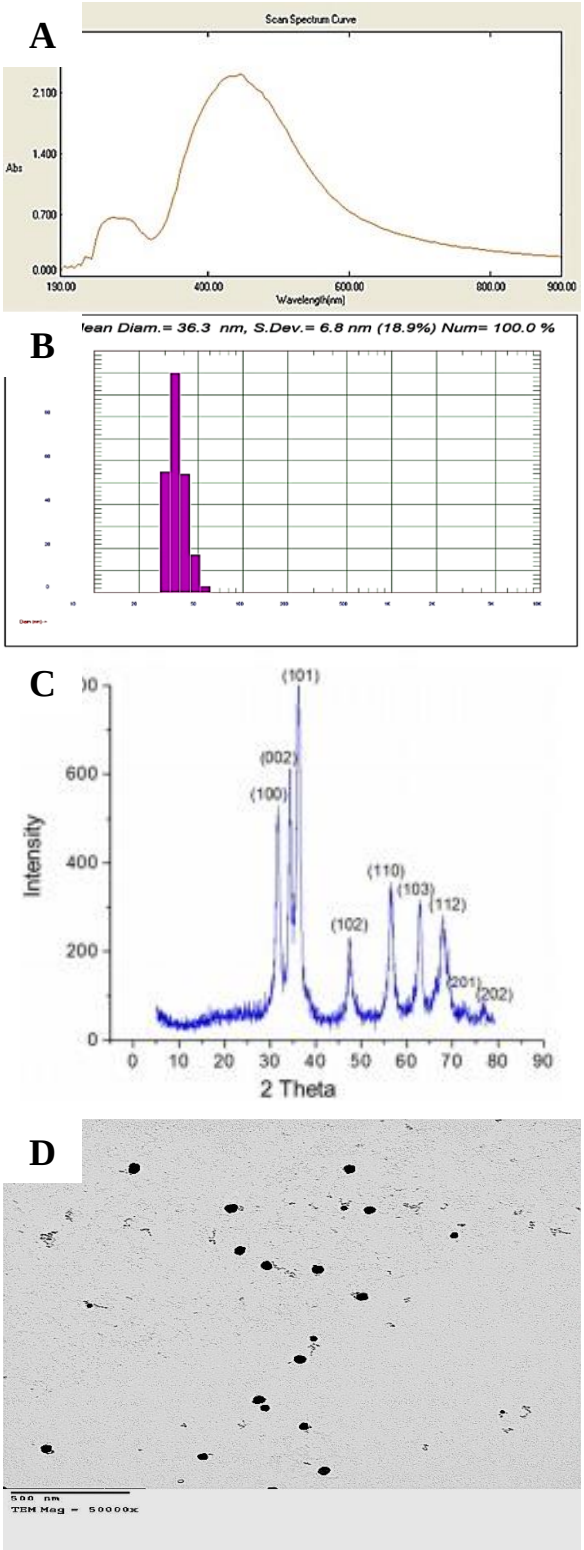

Figure (3) (A) UV-visible spectrum (**B**) DLS pattern of the particle size distribution (**C**) XRD pattern and (**D**) TEM of ZnONPs synthesized using *Streptomyces rochei*,

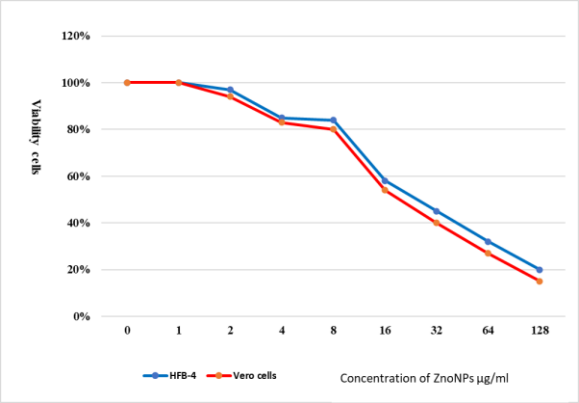

Figure (4) Cytotoxic activity of biosynthesized ZnONPs against HFB-4 and Vero cells

3.5. Immunomodulatory Activity

3. 5. 1. *In vitro* intracellular killing activities

The most promising compound was evaluated against *in vitro* intracellular killing activities using nitro blue tetrazolium (NBT) reduction assay and the obtained results were expressed by percentage (%), where increasing of the percentage led to an improvement in the killing ability of neutrophils that used as innate immunity. In the present study, the immunomodulatory activity of (CFS) of *Streptomyces rochei* and ZnONPs were investigated. As represented in Table (1), intracellular killing activities displayed potency as an immunomodulatory agent with a percentage of 137.2 ± 0.18 and 88.6 ± 0.05 % for both CFS ZnONPs and (CFS) of *Streptomyces rochei*, respectively.

Table (1): Intracellular killing activities of (CFS) and ZnONPs

Compound	Intracellular killing activity %
***Streptomyces rochei*, (C.F.S)**	**88.6 ± 0.05**
ZnONPs	**137.2 ± 0.18**

3. 5. 2. *In vivo* Immunomodulatory investigation

The immunomodulatory activities of the compounds were evaluated by determining their effect on immune organs, thymus, and spleen. There was a significant increase in spleen and thymus weight ($p \leq 0.05$) in ZnONPs treated group compared to the vitamin C group (positive control). There was also a significant change in spleen and thymus indices. ZnONPs had a significantly high thymus index of 0.586 ± 0.02 compared to normal group. while CFS showed activity less than ZnONPs at 0.178 ± 0.14 Table (2). T-lymphocytes were analyzed from peripheral blood and the relative levels of CD4+ and CD8+ T lymphocytes subsets were determined. From the results in Table (3), there was a significant increase in the percentage number of CD4+ T lymphocytes in samples treated with ZnONPs and showed the highest percentage of 85.2 ± 0.07, while CFS showed the lowest percentage with 74.6 ± 0.06 % in comparison with the positive control (treat vitamin C) with a ratio of 76.74 ± 0.7 %. Also, there was a significant increase in the percentage number of CD8+ T lymphocytes in samples treated with ZnONPs and showed the highest percentage with 25.3 ± 0.03%, while CFS exhibited 17.34 ± 0.22 % in comparison with positive control with a ratio of 19.62 ± 0.21 %. No significant changes were noticed in body weight between the control groups and treatment.

3.6. Antimicrobial activity of (CFS) and biosynthesized ZnONPs

The antimicrobial activity of the (CFS) and ZnONPs was investigated against Gram-positive, Gram-negative bacteria, and some fungal strains as shown in Table (4). The inhibition zone of ZnONPs ranges from 15.0 to 28.5mm, while (CFS) exhibits an inhibition zone ranging from 12.0 to 18.0 mm against *Aspergillus niger* and *Staphylococcus aureus* respectively. Moreover, MIC of ZnONPs ranged from 8.67 µg/ml to 125 µg/ml against *Candida albicans* and *Aspergillus niger*, while (CFS) recorded MIC ranging from 62.5 to 250 µg/ml against *Bacillus subtilis* and *Pseudomonas aeruginosa* respectively. Tetracycline and amphotericin B were used as positive control and a single dose of ZnONPs showed stronger potential than the positive control.

Table (2) Effect of compounds on immune organs index.

Index	Normal	Vitamin C 5 mg/kg	CFS	ZnONPs 5 mg/kg
Spleen mg	$90 \pm 0.02^{a*}$	260 ± 0.028^{b}	123 ± 0.015^{c}	$275 \pm .0.64^{d}$
Thymus mg	19.63 ± 0.35^{A}	17.2 ± 0.31^{B}	10.42 ± 0.66^{C}	18.67 ± 0.03^{D}
Spleen index	0.004 ± 0.00^{a}	0.019 ± 0.00^{b}	0.012 ± 0.00^{c}	0.0016 ± 0.00^{d}
Thymus index	0.29 ± 0.26^{A}	0.633 ± 0.06^{B}	0.178 ± 0.14^{C}	0.586 ± 0.02^{D}

*Values share different characters are significantly difference

Table (3) Effect of compounds on T lymphocyte population.

TL Cells %	Normal	Vitamin C 5 mg/kg	CFS	ZnONPs 5 mg/kg
CD4+	$79.82 \pm 1.3^{a**}$	76.74 ± 0.7^{b}	74.6 ± 0.06^{c}	85.2 ± 0.07^{d}
CD8+	18.55 ± 1.9^{A}	19.62 ± 0.21^{AB}	17.34 ± 0.22^{AC}	25.3 ± 0.03^{D}

**Values share different characters are significantly difference

Table (4): Antimicrobial activity of **(CFS) and** ZnONPs

Microbial test strains	Mean diameter of inhibition zone (mm)/ minimum inhibitory concentration (MIC) (µg/ml).							
	Streptomyces rochei, (C.F.S)		ZnONPs		Antibiotics			
					Tetracycline		Amphotericin B	
	Inhibition zone	MIC	Inhibition zone	MIC	Inhibition zone	MIC	Inhibition zone	MIC
***Bacillus subtilis* ATCC 6633**	15±0.40	62.5±0.28	17.5±0.36	31.25 ±0.02	18±0.06	31.25 ±0.17	--	--
***Staphylococcus aureus* ATCC 6538**	18±0.34	125±0.28	28.5±0.34	31.25 ±0.13	27±0.32	62.5± 0.05	--	--
***Escherichia coli* ATCC 7839**	17±0.15	125±0.25	26±0.28	62.5±0.11	32±0.13	31.25 ±0.02	--	--
***Pseudomonas aeruginosa* ATCC 9027**	14 ±0.46	250±0.17	17±0.47	31.25±0.07	20±0.28	15.62 ±0.03	--	--
***Candida albicans* ATCC 10231**	16± 0.41	62.5±0.14	22±0.40	8.67 ±0.15	--	--	19±0.45	15.62±0.05
***Aspergillus niger* RCMB 002007**	12 ± 0.34	125±0.02	15±0.40	125 ±0.85	--	--	16±0.40	62.5 ±0.05
***Aspergillus flavus* ATCC 16883**	--	--	16 ±0.47	62.5 ±0.01	--	--	17 ±0.34	31.25 ±0.01

4. Discussion

The biological activities of ZnONPs have received significant interest worldwide especially by the application of nanotechnology to synthesize particles in the nano scale. The present study highlights the cytotoxic potential, immunomodulatory and antimicrobial activities of biosynthesized ZnONPs. Biosynthesis of nanoparticles provides an eco-friendly and low-cost method. The biological approach for the synthesis of metal nanoparticles includes plants, microorganisms encompassing groups such as bacteria, yeasts, fungi, and actinomycetes as manufactories [36]. Several studies reported the using of cell-free supernatant (CFS) of *Streptomyces* species for biosynthesis of metal nanoparticles [37, 54, 55]. The proteins and amino acids present in the CFS of *Streptomyces rochei* are the key reductants responsible for reduction of zinc nitrate to zinc oxide nanoparticles and may be used as a reducing agent for the synthesis of metal nanoparticles [37, 55]. Characterization of biosynthesized ZnONPs by UV-Visible spectrum exhibits a distinct peak centered around 455nm that is specific for zinc oxide nanoparticles which is due to their large excitation binding energy [56]. It is well known from absorption peak that the bandgap increases by the decreasing in particle size. According to Gupta *et al*., [57] the absorption edge systematically shifts to the lower wavelength or higher energy with the decreasing size of the nanoparticle. The dynamic light scattering (DLS) of ZnONPs exhibits particles size of 36.3 nm. These results disagree with the findings by Debnath *et al*., [58]. The slight difference in ZnONPs particle size may be due to the method used for the synthesis and purification of ZnONPs. Balraj *et al*., [54] reported that the biosynthesized ZnONPs using cell-free supernatant of *Streptomyces* sp. had a spherical shape with a mean diameter of about 20-50 nm. The transmission electron microscopy (TEM) revealed that the biosynthesized ZnONPs are spherical particles within the nano scale ranging from 14.0 nm to 36.0 nm. On the other side, when zinc nitrate is used as a precursor, the spherical ZnONPs are formed and aggregated to form flower-shaped bundles. This aggregation is due to the polarity and electrostatic attraction of zinc nanoparticles. Also, Shabnam *et al*., [59] reported these observations. The particle size obtained from DLS measurements is, of course, larger than the TEM results because DLS analysis measures the hydrodynamic radius [60]. The XRD of ZnONPs showed many different peaks, these diffraction peaks were very similar to peaks obtained by Balraj *et al*., [54], Debnath *et al*., [59].

In vitro cytotoxicity study of ZnONPs on HFB-4 and Vero cells showed that LC_{50} values were 18.5 and 17.3 µg/ml, respectively. The LC_{50} values of ZnONPs were in the range of 1-100 mg/l, in case of ZnO, algae were exceptionally sensitive, and the toxicity of ZnO particles to algae was about 100-fold higher (LC_{50} 0.1 mg/l) than most other organisms [23]. These results are in agreement with LC_{50} recorded by Tianshu *et al*., [61]. The cytotoxicity and superoxide generation were shown *in vitro* curing with ZnONPs above 20µg/ml [62]. The wide range of applications raises concerns concerning their potential toxicity [24]. Also, Salem *et al*., [63] reported that dose (25 mg/kg body weight) of ZnONPs suspension injected in adult rats does not affect the cognitive capacity and neurotransmitters levels. In the present study, the immunomodulatory activity of ZnONPs exhibit intracellular killing activities displayed potency as an immunomodulatory agent with a percentage of 137.2 ± 0.18 by using the nitro blue tetrazolium (NBT) method. One of the broad methods used for determining immune disorders for patients in hospitals is the nitro blue tetrazolium test to measure their immune responses. The reduction of NBT dye provides information about the phagocytic and intracellular killing functions of neutrophils that are important for microbiocidal activity [48-64]. Saptarshi *et al*., [9] demonstrate that sub-cytotoxic doses of ZnONPs can stimulate a strong inflammation. Since zinc is an essential trace element and plays an important role in regulating cellular metabolism, it is also possible that increased exposure to ZnONPs may cause immunomodulation.

In vivo Immunomodulatory activity of ZnONPs on immune organs, thymus and spleen revealed significant increase in spleen and thymus weight ($p \leq 0.05$) and significant change in spleen and thymus indices. ZnONPs had a significantly high thymus index of 0.586 ±0.02. Jitendra *et al*., [58] demonstrate that concentrations less than 50mg/kg of ZnONPs showed immunomodulatory effects. Our results revealed a significant increase in the percentage of CD4+ T lymphocytes in samples treated with ZnONPs with highest percentage of 85.2 ± 0.07 and an increase in the percentage of CD8+ T lymphocytes with a percentage of 25.3 ± 0.03. The role of nanoparticles in macrophages' phagocytic activity was underlined by Paul *et al*., [66]. No significant changes were noticed in body weight between the control groups and treatment. Comparing with the control groups, the mice were given 50 mg/kg of ZnONPs exhibited an increase in the absolute weights of the spleen due to immunological overload on the spleen [65]. Saptarshi *et al*., [9] demonstrate that ZnONPs are a strong immune stimulator.

The antimicrobial activity of ZnONPs exhibits inhibition zone ranging from 15.0 to 28.5mm, against *Aspergillus niger* and *Staphylococcus aureus* and MIC ranging from 8.67 µg/ml to 125 µg/ml against *Candida albicans* and *Aspergillus niger*, respectively. Iqbal *et al*., [67] reported antimicrobial activity of ZnONPs with MIC 37.5µg/ml against *E. coli* ATCC 15224, *Staphylococcus. aureus* ATCC 25923, *Klebsiella pneumonia* ATCC 4617, *Bacillus subtilis* ATCC 6633 *Aspergillus niger* FCBP 0918 and 75, 150µg/ml against *Pseudomonas aeruginosa* ATCC 9721 and *Aspergillus flavus* FCBP 0064, respectively. The direct contact of ZnONPs with the bacterial cell and the production of reactive oxygen species (ROS) close to the bacterial membrane that causes damage to bacterial cells has also been suggested to be the other mechanism [68]. First, the cell wall of the bacteria and then the oxidative damage proceeds to the inner cytoplasmic membrane and peptidoglycan layer. Affecting the respiratory activities, slow leakage of RNA and proteins and rapid leakage of K^+ ions are believed to be the primary reason for bacterial death. The global negative charge of the bacterial cells at the biological pH occurred due to the dissociation of carboxylic groups [69], while ZnO has positively charged properties at the zeta potential of +24 mV. The interaction/electrostatic force that occurred between negatively charged bacterial cells and positively charged ZnO leads to disruption of the cell wall and damage occurred by entering the cell [68]. Brayner *et al*., [70] showed that the interaction between *E. coli* cells and ZnONPs yields cell wall disorganization and subsequently internalization of NPs into the cells. They recognized fundamental damage to *E. coli* with disorganized cell walls by SEM images which showed the changed morphology, a consequence of intracellular content leakage. Likewise, the images revealed that ZnONPs are both outside and inside the cell bordered probably by lipopolysaccharides released by bacteria. They demonstrate the capability of ZnONPs to decrease the bacterial growth. It was attributed to membrane perturbation and raising of its permeability, which in turn causes the gathering of ZnONPs inside the membrane and then reaches the cytoplasm [70].

5. Conclusion

In summary, a rapid method for extracellular synthesis of metallic ZnONPs using cell-free filtered (CF) of *Streptomyces rochei*, was demonstrated. The synthesized ZnONPs were characterized by UV–Vis spectra, DLS, TEM and XRD. ZnONPs were highly stable and crystalline which was confirmed by the XRD pattern. The synthesized ZnONPs had shown the best antimicrobial efficacy on both Gram-positive, Gram-negative bacteria and some fungi. ZnONPs showed a significant immunostimulatory effect and intracellular killing activities potency with a percentage of 137.2 ± 0.18 % and with a percentage for CD4+ and CD8+ of 85.2 ± 0.07% and 25.3 ± 0.03 %, respectively. The present study has opened a possible way for synthesizing ZnONPs against

microbial pathogens using natural biomolecules which could be used in the pharmaceutical industry.

Acknowledgments
Not applicable.

Conflicts
The author has no conflicts of interest that are concerned with this article.

Ethics approval and consent to participate
Not applicable.

Consent for publication
Not applicable.

Funding
N/A

Availability of data and materials
Not applicable.
Author Contributions Statement

G.M.E.-S. and A.R.A. conceived the presented idea, co-wrote the paper, and supervised the research. D. M A. and A.S.E.H. isolation, identification of *Streptomyces*, biosynthesis, characterization of nanoparticles. A.A.A performed determination of minimum inhibitory concentrations (MIC) and immunomodulatory activity Finally, all authors discussed the results, commented, and revised the manuscript

References

1. Abou El-Kheir, A. and El-Gabry, L.K. (2022). Potential Applications of Nanotechnology In Functionalization of Synthetic Fibres (A Review). *Egyptian Journal of Chemistry*, *65*(9), pp.5-6.
2. Abdelhak, A., Ghanem, A.F., Abdulaziz, A., Kabel, K., Noah, A.Z., Youssef, A. and Dahab, A.S. (2022). Synthesis and Evaluation of Poly (isobutylene-alt-maleic anhydride)-co-Poly (ethylene glycol) and its Copper Oxide Nanocomposite for Enhancing the Performance of Water-based Drilling Fluids in HPHT Wells. *Egyptian Journal of Chemistry*, 65(9), pp.2-4.
3. Sarhan, A., Abdelghany, A.M. and El-Dossoki, F. (2022). Synthesis and characterization of nano CuO/ZnO/Al2O3 catalyst via Laser ablation route for the preparation of some cyanoacetani-lide derivatives. *Egyptian Journal of Chemistry*, *65*(7), pp.275-279.
4. RM, S., Abdel-Razik, A.B., Ebeed, N.M., Esmail, R.M. and Taha, E.H. (2022). Impact of engineered nano silver on root-knot nematode, *Meloidogyne incognita* and on DNA damage in tomato plants under screen house conditions. *Egyptian Journal of Chemistry*, *65*(3), pp.1-2.
5. Elseidy, A., Bashandy, S.A., Ibrahim, F.A., El-Rahman, A., Sahar, S., Farid, O., Moussa, S. and El-Baset, M.A. (2022). Zinc oxide nanoparticles characterization and therapeutic evaluation on high fat/sucrose diet induced-obesity. *Egyptian Journal of Chemistry*, 65(9), pp.1-3.
6. Banoon, S.R. and Ghasemian, A. (2021). The characters of graphene oxide nanoparticles and doxorubicin against HCT-116 colorectal cancer cells *in vitro*. *Journal of Gastrointestinal Cancer*, pp.1-5.
7. Aldujaili, N.H. and Banoon, S.R. (2020). Antibacterial characterization of titanium nanoparticles nano synthesized by *Streptococcus thermophilus*. *Periodico Tche Quimica (Online)*, *17*(34), pp.311-320.
8. Wang, Z. L. (2004). Zinc oxide nanostructures: growth, properties and applications. *Journal of physics: condensed matter*, 16(25), R829.
9. Saptarshi, S. R., Duschl, A., & Lopata, A. L. (2013). Interaction of nanoparticles with proteins: relation to bio-reactivity of the nanoparticle. *Journal of nanobiotechnology*, 11(1), 1-12.
10. Bisht, G., & Rayamajhi, S. (2016). ZnO Nanoparticles: A Promising Anticancer Agent. *Nanobiomedicine*. https://doi.org/10.5772/63437.
11. Mohd Yusof, H., Mohamad, R., Zaidan, U. H., & Rahman, A. (2019). Microbial synthesis of zinc oxide nanoparticles and their potential application as an antimicrobial agent and a feed supplement in animal industry: a review. *Journal of animal science and biotechnology*, *10*(1), 1-22.
12. Shahid, S., Fatima, U., Sajjad, R., & Khan, S. A. (2019). Bioinspired nanotheranostic agent: Zinc oxide; green synthesis and biomedical potential. *Dig. J. Nanomater. Biostruct*, *14*, 1023-1031.
13. Karlsson, H. L., Cronholm, P., Gustafsson, J., & Moller, L. (2008). Copper oxide nanoparticles are highly toxic: a comparison between metal oxide nanoparticles and carbon nanotubes. *Chemical research in toxicology*, *21*(9), 1726-1732.
14. Lin, W., Xu, Y., Huang, C. C., Ma, Y., Shannon, K. B., Chen, D. R., & Huang, Y. W. (2009). Toxicity of nano-and micro-sized ZnO particles in human lung epithelial cells. *Journal of Nanoparticle Research*, *11*(1), 25-39.
15. Feltis, B. N., O'Keefe, S. J., Harford, A. J., Piva, T. J., Turney, T. W., & Wright, P. F. (2012). Independent cytotoxic and inflammatory responses to zinc oxide nanoparticles in human

monocytes and macrophages. *Nanotoxicology*, *6*(7), 757-765.
16. Kang, T., Guan, R., Chen, X., Song, Y., Jiang, H., & Zhao, J. (2013). In vitro toxicity of different-sized ZnO nanoparticles in Caco-2 cells. *Nanoscale research letters*, *8*(1), 1-8.
17. Prach, M., Stone, V., & Proudfoot, L. (2013). Zinc oxide nanoparticles and monocytes: impact of size, charge and solubility on activation status. *Toxicology and applied pharmacology*, *266*(1), 19-26.
18. Amy M. Holmes, Lorraine Mackenzie & Michael S. Roberts (2020) Disposition and measured toxicity of zinc oxide nanoparticles and zinc ions against keratinocytes in cell culture and viable human epidermis, *Nanotoxicology*, 14:2, 263-274, DOI: 10.1080/17435390.2019.1692382
19. Ahamed, M., Akhtar, M. J., Raja, M., Ahmad, I., Siddiqui, M. K., AlSalhi, M. S., & Alrokayan, S. A. (2011). ZnO nanorod-induced apoptosis in human alveolar adenocarcinoma cells via p53, survivin and bax/bcl-2 pathways: role of oxidative stress. *Nanomedicine: nanotechnology, biology, and medicine*, *7*(6), 904–913. https://doi.org/10.1016/j.nano.2011.04.011.
20. Andersson-Willman, B., Gehrmann, U., Cansu, Z., Buerki-Thurnherr, T., Krug, H. F., Gabrielsson, S., & Scheynius, A. (2012). Effects of subtoxic concentrations of TiO2 and ZnO nanoparticles on human lymphocytes, dendritic cells and exosome production. *Toxicology and applied pharmacology*, *264*(1), 94-103.
21. Guo, D., Bi, H., Liu, B., Wu, Q., Wang, D., & Cui, Y. (2013). Reactive oxygen species-induced cytotoxic effects of zinc oxide nanoparticles in rat retinal ganglion cells. *Toxicology in Vitro*, *27*(2), 731-738.
22. Yang, H., Liu, C., Yang, D., Zhang, H., & Xi, Z. (2009). Comparative study of cytotoxicity, oxidative stress and genotoxicity induced by four typical nanomaterials: the role of particle size, shape and composition. *Journal of applied Toxicology*, *29*(1), 69-78.
23. Ivask, A., Juganson, K., Bondarenko, O., Mortimer, M., Aruoja, V., Kasemets, K., ... & Kahru, A. (2014). Mechanisms of toxic action of Ag, ZnO and CuO nanoparticles to selected ecotoxicological test organisms and mammalian cells in vitro: a comparative review. *Nanotoxicology*, *8*(sup1), 57-71.
24. Singh, S. (2019). Zinc oxide nanoparticles impacts cytotoxicity, genotoxicity, developmental toxicity, and neurotoxicity. *Toxicology mechanisms and methods*, *29*(4), 300-311.
25. Xia, T., Kovochich, M., Liong, M., Madler, L., Gilbert, B., Shi, H., ... & Nel, A. E. (2008). Comparison of the mechanism of toxicity of zinc oxide and cerium oxide nanoparticles based on dissolution and oxidative stress properties. *ACS nano*, *2*(10), 2121-2134.
26. Buerki-Thurnherr, T., Xiao, L., Diener, L., Arslan, O., Hirsch, C., Maeder-Althaus, X., ... & Krug, H. F. (2013). In vitro mechanistic study towards a better understanding of ZnO nanoparticle toxicity. *Nanotoxicology*, *7*(4), 402-416.
27. Song, W., Zhang, J., Guo, J., Zhang, J., Ding, F., Li, L., & Sun, Z. (2010). Role of the dissolved zinc ion and reactive oxygen species in cytotoxicity of ZnO nanoparticles. *Toxicology letters*, *199*(3), 389-397.
28. Qureshi, N. A., & Afridi, R. (2018). Comparative analysis of egg adapted vaccines and salinomycin against coccidiosis in chicks. *Microbial pathogenesis*, *123*, 454-460.
29. Abd Elkodous, M., El-Sayyad, G. S., Abdel Maksoud, M. I. A., Abdelrahman, I. Y., Mosallam, F. M., Gobara, M., & El-Batal, A. I. (2020). Fabrication of ultra-pure anisotropic zinc oxide nanoparticles via simple and cost-effective route: implications for UTI and EAC medications. *Biological trace element research*, *196*(1), 297-317.
30. Gao, Y., Arokia Vijaya Anand, M., Ramachandran, V., Karthikkumar, V., Shalini, V., Vijayalakshmi, S., & Ernest, D. (2019). Biofabrication of Zinc Oxide Nanoparticles from Aspergillus niger, Their Antioxidant, Antimicrobial and Anticancer Activity. *Journal of Cluster Science*, *30*, 937-946.
31. Huang, J., Liu, J., & Wang, J. (2020). Optical properties of biomass-derived nanomaterials for sensing, catalytic, biomedical and environmental applications. *TrAC Trends in Analytical Chemistry*, *124*, 115800.
32. Wang, Y., Zhang, Q., Zhang, C. L., & Li, P. (2012). Characterisation and cooperative antimicrobial properties of chitosan/nano-ZnO composite nanofibrous membranes. *Food Chemistry*, *132*(1), 419-427.
33. Makaremi, M., Lim, C. X., Pasbakhsh, P., Lee, S. M., Goh, K. L., Chang, H., & Chan, E. S. (2016). Electrospun functionalized polyacrylonitrile–chitosan Bi-layer membranes for water filtration applications. *RSC advances*, *6*(59), 53882-53893.
34. Sahu, A., Kwon, I., & Tae, G. (2020). Improving cancer therapy through the nanomaterials-assisted alleviation of hypoxia. *Biomaterials*, *228*, 119578.

35. Salem, M. A., Ragab, A., Askar, A. A., El-Khalafawy, A., & Makhlouf, A. H. (2020). One-pot synthesis and molecular docking of some new spiropyranindol-2-one derivatives as immunomodulatory agents and in vitro antimicrobial potential with DNA gyrase inhibitor. *European Journal of Medicinal Chemistry*, *188*, 111977.
36. El-Batal, A. I., Amin, M. A., Shehata, M. M., & Hallol, M. M. (2013). Synthesis of silver nanoparticles by Bacillus stearothermophilus using gamma radiation and their antimicrobial activity. *World Appl Sci J*, *22*(1), 01-16.
37. Sivalingam, P., Antony, J. J., Siva, D., Achiraman, S., & Anbarasu, K. (2012). Mangrove Streptomyces sp. BDUKAS10 as nanofactory for fabrication of bactericidal silver nanoparticles. *Colloids and Surfaces B: Biointerfaces*, *98*, 12-17.
38. Tresner, H. D., Davies, M. C., & Backus, E. J. (1961). Electron microscopy of Streptomyces spore morphology and its role in species differentiation. *Journal of Bacteriology*, *81*(1), 70-80.
39. Shirling, E.B., & Gottlieb, D. (1966). Methods for characterization of Streptomyces species. *International Journal of Systematic and Evolutionary Microbiology*, *16*, 313-340.
40. Darwesh, O. M., Elsehemy, I. A., El-Sayed, M. H., El-Ghamry, A. A., & El-Hawary, A. S. (2020). *Thermoflavimicrobium dichotomicum* as a novel thermoalkaliphile for production of environmental and industrial enzymes. *Biointerface Research in Applied Chemistry*, *10*, 4811-4820.
41. Kämpfer, P., Kroppenstedt, R. M., & Dott, W. (1991). A numerical classification of the genera Streptomyces and Streptoverticillium using miniaturized physiological tests. *Microbiology*, *137*(8), 1831-1891.
42. Liu, W., Sun, Z., Zhang, J., Gao, W., Wang, W., Wu, L., ... & Zhang, H. (2009). Analysis of microbial composition in acid whey for dairy fan making in Yunnan by conventional method and 16S rRNA sequencing. *Current microbiology*, *59*(2), 199-205.
43. Kumar, S., Stecher, G., Li, M., Knyaz, C., & Tamura, K. (2018). MEGA X: molecular evolutionary genetics analysis across computing platforms. *Molecular biology and evolution*, *35*(6), 1547.
44. Waksman S. (1961). Book: The Actinomycetes, 2, classification, identification and descriptions of genera and species. *The Williams and Wilkins Company, Baltimore*.
45. Selvakumar, P., Viveka, S., Prakash, S., Jasminebeaula, S., & Uloganathan, R. (2012). Antimicrobial activity of extracellularly synthesized silver nanoparticles from marine derived *Streptomyces rochei*. *Int. J. Pharm. Biol. Sci*, *3*(3), 188-197.
46. Zare, E., Pourseyedi, S., Khatami, M., & Darezereshki, E. (2017). Simple biosynthesis of zinc oxide nanoparticles using nature's source, and it's in vitro bio-activity. *Journal of Molecular Structure*, *1146*, 96-103.
47. Abu-Serie, M. M., & El-Fakharany, E. M. (2017). Efficiency of novel nanocombinations of bovine milk proteins (lactoperoxidase and lactoferrin) for combating different human cancer cell lines. *Scientific reports*, *7*(1), 1-12.
48. Akbay, P., Calis, I., Ündeger, Ü., Basaran, N., & Basaran, A. A. (2002). *In vitro* immunomodulatory activity of verbascoside from *Nepeta ucrainica L*. *Phytotherapy Research: An International Journal Devoted to Pharmacological and Toxicological Evaluation of Natural Product Derivatives*, *16*(6), 593-595.
49. Akbay, P., Basaran, A. A., Undeger, U., & Basaran, N. (2003). In vitro immunomodulatory activity of flavonoid glycosides from Urtica dioica L. *Phytotherapy Research: An International Journal Devoted to Pharmacological and Toxicological Evaluation of Natural Product Derivatives*, *17*(1), 34-37.
50. Ayeka, P. A., Bian, Y., Githaiga, P. M., & Zhao, Y. (2017). The immunomodulatory activities of licorice polysaccharides (Glycyrrhiza uralensis Fisch.) in CT 26 tumor-bearing mice. *BMC Complementary and Alternative Medicine*, *17*(1), 1-9.
51. Zhang, W. N., Gong, L. L., Liu, Y., Zhou, Z. B., Wan, C. X., Xu, J. J., ... & Chen, Y. (2020). Immunoenhancement effect of crude polysaccharides of *Helvella leucopus* on cyclophosphamide-induced immunosuppressive mice. *Journal of Functional Foods*, *69*, 103942.
52. Wu, R. Y. (1984). Studies on the Streptomyces SC4. II Taxonomic and biological characteristics of Streptomyces strain SC4. *Bot Bull Acad Sin*, *25*, 111-123.
53. Spatz C. (1993). Book: Basic Statistics, 5th ed., *Brooks/Cole Publ. Co*., California, USA, 135-161.
54. Balraj, B., Senthilkumar, N., Siva, C., Krithikadevi, R., Julie, A., Potheher, I. V., & Arulmozhi, M. (2017). Synthesis and characterization of zinc oxide nanoparticles using marine Streptomyces sp. with its investigations on anticancer and antibacterial activity. *Research on Chemical Intermediates*, *43*(4), 2367-2376.
55. Bukhari, S. I., Hamed, M. M., Al-Agamy, M. H., Gazwi, H. S., Radwan, H. H., & Youssif, A.

M. (2021). Biosynthesis of copper oxide nanoparticles using *Streptomyces MHM38* and its biological applications. *Journal of Nanomaterials*, *2021*.

56. Dobrucka, R., & Długaszewska, J. (2016). Biosynthesis and antibacterial activity of ZnO nanoparticles using *Trifolium pratense* flower extract. *Saudi journal of biological sciences*, *23*(4), 517-523.
57. Gupta, A., Srivastava, P., Bahadur, L., Amalnerkar, D. P., & Chauhan, R. (2015). Comparison of physical and electrochemical properties of ZnO prepared via different surfactant-assisted precipitation routes. *Applied Nanoscience*, *5*(7), 787-794.
58. Debnath, P., Sen, K., Mondal, A., Mondal, A., & Mondal, N. K. (2021). Insight into Photocatalytic Degradation of Amoxicillin by Biofabricated Granular Zinc Oxide Nanoparticle: Mechanism, Optimization and Toxicity Evaluation. *International Journal of Environmental Research*, *15*(3), 571-583.
59. Fakhari, S., Jamzad, M., & Kabiri Fard, H. (2019). Green synthesis of zinc oxide nanoparticles: a comparison. *Green chemistry letters and reviews*, *12*(1), 19-24.
60. El-Batal, A. I., Mona, S. S., & Al-Tamie, M. S. S. (2015). Biosynthesis of gold nanoparticles using marine *Streptomyces cyaneus* and their antimicrobial, antioxidant and antitumor (in vitro) activities. *J. Chem. Pharm. Res*, *7*(7), 1020-1036.
61. Kang, T., Guan, R., Chen, X., Song, Y., Jiang, H., & Zhao, J. (2013). In vitro toxicity of different-sized ZnO nanoparticles in Caco-2 cells. *Nanoscale research letters*, *8*(1), 1-8.
62. Li, C. H., Shen, C. C., Cheng, Y. W., Huang, S. H., Wu, C. C., Kao, C. C., ... & Kang, J. J. (2012). Organ biodistribution, clearance, and genotoxicity of orally administered zinc oxide nanoparticles in mice. *Nanotoxicology*, *6*(7), 746-756.
63. Amara, S., Ben-Slama, I., Mrad, I., Rihane, N., Jeljeli, M., El-Mir, L., ... & Sakly, M. (2014). Acute exposure to zinc oxide nanoparticles does not affect the cognitive capacity and neurotransmitters levels in adult rats. *Nanotoxicology*, *8*(sup1), 208-215.
64. Askar, A. A., Selim, M. S., El-Safty, S. A., Hashem, A. I., Selim, M. M., & Shenashen, M. A. (2021). Antimicrobial and immunomodulatory potential of nanoscale hierarchical one-dimensional zinc oxide and silicon carbide materials. *Materials Chemistry and Physics*, *263*, 124376.
65. Kumar, J., Mitra, M. D., Hussain, A., & Kaul, G. (2019). Exploration of immunomodulatory and protective effect of *Withania somnifera* on trace metal oxide (zinc oxide nanoparticles) induced toxicity in Balb/c mice. *Molecular biology reports*, *46*(2), 2447-2459.
66. Paul, D., Achouri, S., Yoon, Y. Z., Herre, J., Bryant, C. E., & Cicuta, P. (2013). Phagocytosis dynamics depends on target shape. *Biophysical journal*, *105*(5), 1143-1150.
67. Iqbal, J., Abbasi, B. A., Yaseen, T., Zahra, S. A., Shahbaz, A., Shah, S. A., ... & Ahmad, P. (2021). Green synthesis of zinc oxide nanoparticles using *Elaeagnus angustifolia L.* leaf extracts and their multiple in vitro biological applications. *Scientific Reports*, *11*(1), 1-13.
68. Lin, H., Yang, M., Tang, H., & Pan, F. (2018). Effect of minor Sc on the microstructure and mechanical properties of AZ91 Magnesium Alloy. *Progress in Natural Science: Materials International*, *28*(1), 66-73.
69. Brayner, R., Ferrari-Iliou, R., Brivois, N., Djediat, S., Benedetti, M. F., & Fiévet, F. (2006). Toxicological impact studies based on *Escherichia coli* bacteria in ultrafine ZnO nanoparticles colloidal medium. *Nano letters*, *6*(4), 866-870.
70. Stiomenov, P. K., Klinger, R. L., Marchin, G. L., & Klabunde, K. J. (2002). Metal oxide nanoparticles as bacterial agents. *Langmuir*, *18*(17), 6679-6686.

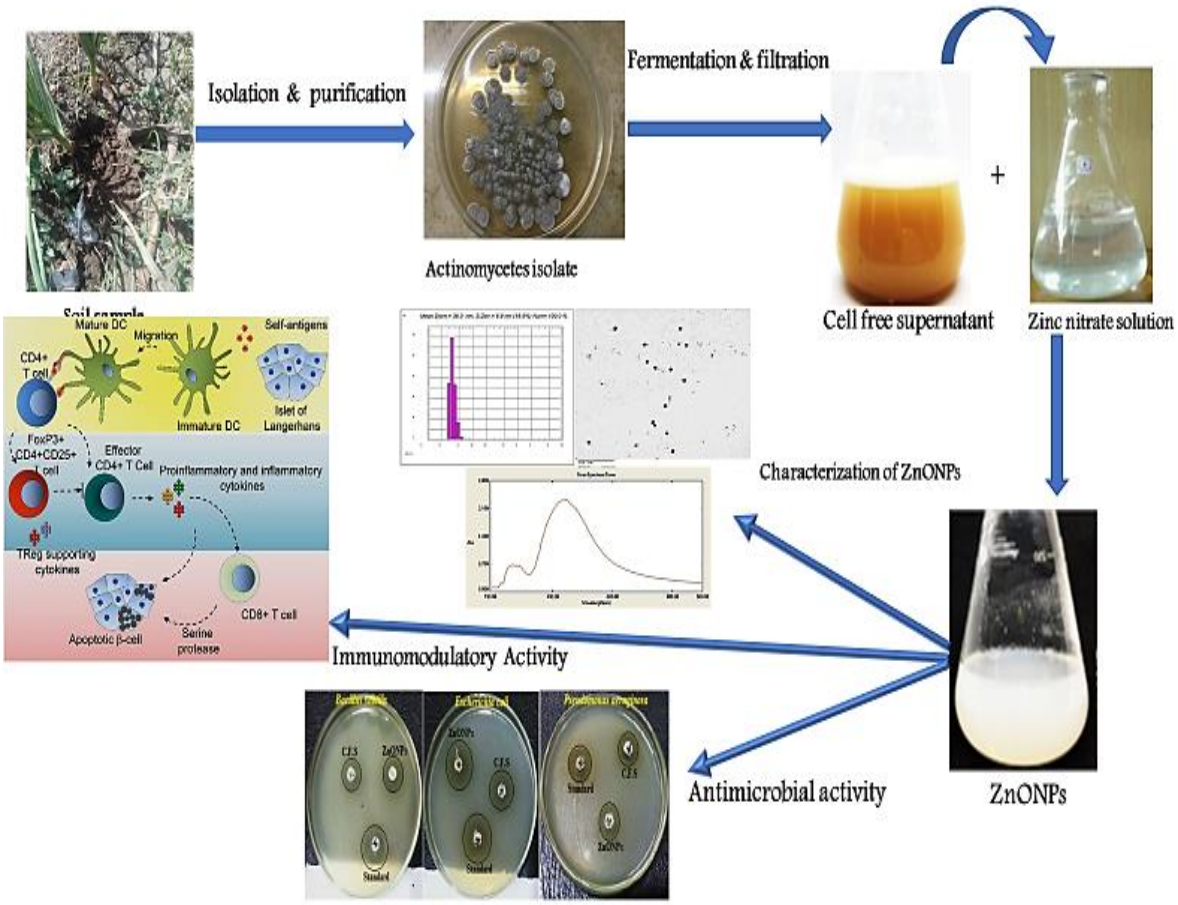

Graphical Abstract